

KINETICS OF THE HYDROGEN-EVOLUTION REACTION ON PALLADIUM ELECTRODES IN MOLTEN POTASSIUM BISULPHATE*

A. J. ARVIA, A. J. CALANDRA and H. A. VIDELA

Instituto Superior de Investigaciones, Facultad de Química y Farmacia,
and Universidad Nacional de La Plata, La Plata, Argentina

Abstract—The kinetics of the electrochemical formation of hydrogen on differently prepared palladium electrodes in the electrolysis of molten potassium bisulphate has been studied in the temperature range 240 to 330°C. Current/voltage curves fit two limiting Tafel lines having slopes of $2.3(RT/2F)$ and $2.3(2RT/F)$ respectively.

Semilogarithmic plots of decay curves exhibit a limiting region of slope $2.3(RT/2F)$. At high temperature an interference due to permeation of hydrogen in the metal during the decay process is observed, particularly noticeable when bright palladium electrodes are used.

The kinetics of the electrochemical process is interpreted, on the basis that the α -Pd-H system predominates, the rate-determining step being the combination of hydrogen atoms on the electrode surface, at least at low overvoltages. At higher ones the ion-plus-atom reaction can account for the experimental results.

Résumé—On a étudié la cinétique de la formation électrochimique de l'hydrogène sur des électrodes de palladium préparées de diverses manières pendant l'électrolyse du sulfate acide de potassium à des températures entre 240 et 330°C. Les courbes de polarisation suivent deux lignes limites de Tafel avec des pentes de $2,3(RT/2F)$ et $2,3(2RT/F)$ respectivement.

La représentation surtension/log(temp) montrent une région limite avec une pente de $2,3(RT/2F)$. A des températures élevées on a observé l'interférence de la perméabilité de l'hydrogène dans le métal au cours du processus de décroissance du potentiel, particulièrement apparente quand des électrodes de palladium poli furent employées.

La cinétique du processus électrochimique a été interprétée en supposant que le système α -Pd-H predomine et la réaction régulatrice est la recombinaison des atomes d'hydrogène sur la surface de l'électrode au moins pour de basses surtensions. A des surtensions élevées la réaction de l'ion plus l'atome permet d'expliquer les résultats expérimentaux.

Zusammenfassung—Die Kinetik der Wasserstoffabscheidung an verschiedenartig präparierten Palladiumelektroden bei der Elektrolyse von geschmolzenem Kaliumbisulfat wurde bei Temperaturen zwischen 240 und 330°C untersucht. Die Strom/Spannungskurven stimmen mit zwei Grenz-Tafelgeraden der Steigung $2,3(RT/2F)$ bzw. $2,3(2RT/F)$ überein.

Semilogarithmische Darstellungen des zeitlichen Potentialverlaufs weisen ein Grenzgebiet mit einer Steigung von $2,3(RT/2F)$ auf. Bei hohen Temperaturen kann Interferenz beobachtet werden, welche durch das Eindringen von Wasserstoff in das Metall während der Potentialabnahme verursacht wird. Dieser Effekt ist besonders ausgeprägt wenn man glänzende Palladiumelektroden verwendet. Die Kinetik des elektrochemischen Vorganges wird in der Weise gedeutet, dass bei vorherrschendem α -Pd-H System die Rekombination der Wasserstoffatome an der Oberfläche zumindest bei kleinen Überspannungen den geschwindigkeitsbestimmenden Schritt darstellt. Bei höheren Überspannungen haben die Reaktionen der Ionen und der Atome einen Einfluss auf die experimentellen Ergebnisse.

INTRODUCTION

AFTER studying the electrochemical formation of hydrogen during the electrolysis of molten bisulphates on platinum^{1,2} and gold electrodes,³ it was interesting to continue the investigation on palladium electrodes. These electrodes are of special interest because their behaviour is determined by the properties of adsorbed atomic hydrogen as well as dissolved hydrogen.

The absorption of gaseous hydrogen from aqueous electrolytic solutions led to the

* Manuscript received 1 January 1968.

establishment of the Pd-H-H₂ system which has been extensively studied.⁴⁻⁷ Reference electrodes related to the Pd-H system in aqueous solutions were employed by several workers^{8,9} and the literature about this was reviewed some years ago.¹⁰

Hydrogen dissolves in palladium according to the $p^{\frac{1}{2}}$ law at high temperatures and low pressures.¹¹⁻¹³ Deviations from this law occur both for hydrogen and deuterium lower than 600°C, or pressures higher than 1 atm. At 295°C and pressure about 20 atm, a critical point exists below which the pressure isotherms show that two solid phases are present. The phase diagram for the palladium-hydrogen system exhibits three regions of solid solutions: the α -Pd-H system related to low hydrogen content in the metal and high temperature, in which there are positive holes in the palladium d-bands; the β -Pd-H system, in which the palladium d-bands are completely filled with electrons from hydrogen atoms (H/Pd \approx 0.6), and the interval of immiscibility or ($\alpha + \beta$) region. At the critical temperature the α and β systems, which are both fcc and differ only in the magnitudes of their lattice constants, coalesce.^{14,15}

The literature about the electrochemical behaviour of the Pd-H systems in aqueous solutions has been reviewed recently,¹⁶ particularly in connexion with the phase transition and adsorption phenomena. At room temperature the thermodynamic and kinetic studies refer preferentially to the β -Pd-H system.¹⁶⁻²² The α -Pd-H system has not been so extensively considered, although the electrochemical kinetics of the electrode has been studied at room temperature by means of a palladium bi-electrode.²³

A qualitative study of the oxidation of hydrogen on a palladium electrode at 500°C in chloride melts has been performed, particularly directed to obtain a hydrogen-diffusion electrode for fuel cells,²⁴ and anodic polarization curves were also obtained for diffusion palladium-hydrogen electrodes in eutectic mixtures of alkali molten carbonates,²⁵ but these electrodes have not yet been studied from the view point of fundamental electrode kinetics and in the presence of hydrogen-ion-containing melts such as potassium bisulphate.

The present investigation is a continuation of the previous series of studies on the electrochemistry of molten bisulphates. Here, the palladium electrodes are used at temperatures above the melting point of the melt and under 1 atm pressure hydrogen gas, so that according to the phase diagram of the Pd-H system^{14,26} only the α -phase is present and the transition region is not included. This being the case, the behaviour of the palladium electrodes should be comparable to the corresponding α -Pd-H electrodes in aqueous solutions and to electrodes such as platinum and gold where hydrogen permeation is low. Nevertheless the high rate of diffusion of hydrogen within palladium, particularly at high temperature, will reflect on the electrode potentials both at open circuit and during non-steady measurements.

EXPERIMENTAL TECHNIQUE

The electrolysis cell was similar to that described in previous publications.^{1,2} A hydrogen reversible electrode was used as reference; it was formed with a platinized platinum sheet dipped into the melt and saturated with hydrogen gas, at atmospheric pressure, in a conventional Luggin-Haber capillary arrangement. Three different types of cathodes were employed as working electrodes (i) bright palladium electrodes (ii) palladized palladium electrodes obtained by electrolysing a palladizing solution²⁷ on a palladium base, at room temperature and at a cd of 0.030 A/cm² (iii) palladized platinum electrodes prepared similarly as in (ii) but on a platinum base. Wire or sheet

electrodes were used indifferently, with an apparent area between 1 and 3 cm². A platinum sheet properly separated in an anodic section was used as counter-electrode.

Purified and carefully desiccated Mallinckrodt potassium bisulphate was used as electrolyte, saturated either with nitrogen or hydrogen by bubbling the gas through it. Thus, a controlled atmosphere was maintained inside the cell, and at the same time the electrolyte was continuously stirred. The experiments covered the temperature range from 240 to 330°C.

Before recording any experimental data, the working electrodes were used as cathodes until a reproducible and stable rest potential was achieved. Steady current/voltage curves were determined either galvanostatically or potentiostatically, covering a range of apparent current density from 10 μA to 100 mA/cm², the current being changed upwards and downwards.

These curves were properly corrected for the pseudo-ohmic drop, the latter being determined by non-steady measurements, comprising the evolution of the overvoltage either when the current was switched on at constant cd or at current interruption.

RESULTS

When potassium bisulphate is electrolysed on palladium cathodes hydrogen is evolved, with a current efficiency close to 100% particularly at cds lower than 10 mA/cm², as is the case for platinum and gold electrodes. At larger cds minor amounts of sulphur formation were observed.

The experimental results depend principally on the type of electrode used and on temperature.

Palladized-palladium electrodes

A set of current/voltage curves obtained either galvanostatically or potentiostatically at low temperature is shown in Fig. 1 in a semilogarithmic plot. The overvoltage

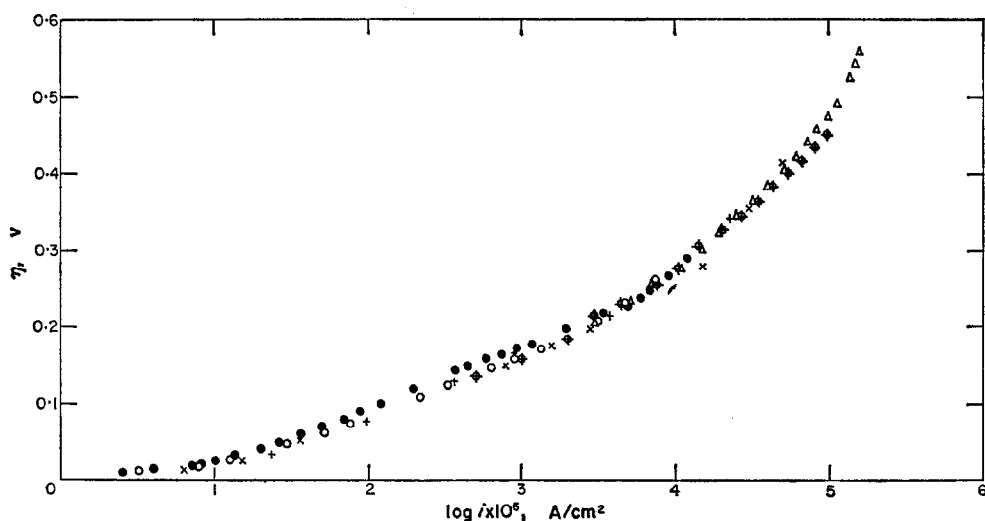


FIG. 1. Tafel plots for palladized-palladium electrodes, 254°C.
Results from different runs; ○, potentiostatic run.

η is defined as the difference between the electrode potential E when a current I flows through the cell, and the rest potential of the working electrode E_r , both measured against the hydrogen reference electrode, and considering the pseudo-ohmic drop correction. The current density i is referred to the apparent electrode area.

The experimental data at low temperature can be well approximated by two straight lines. The first covers an overvoltage range from about 0.04 to 0.20 V, and has a slope near to $2.3(RT/2F)$. The second line extends up from about 0.25 to 0.50 V, and its slope is about 2.5 times that of the former. At the highest cds the overvoltage increases rather more rapidly. This effect, already observed on platinum and gold electrodes, may be largely related to the higher rate of bubble formation and the decrease of the actual reaction surface.

As temperature increases, there is an appreciable overvoltage decrease, as shown in Figs. 2 and 3. At 272°C the two slopes still exist. At 323°C, the overvoltage is much lower and a Tafel slope close to $2.3(RT/F)$ is exhibited, at high overvoltages.

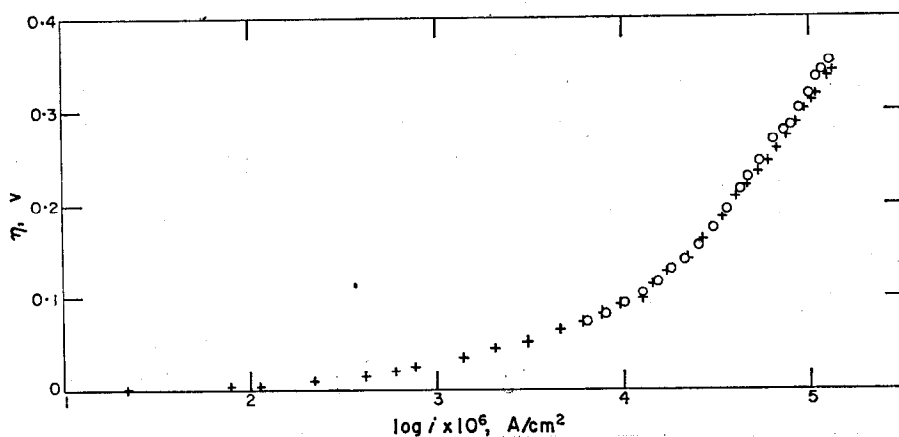


FIG. 2. Tafel plots for palladized-palladium electrodes, 272°C.
Results from different runs.

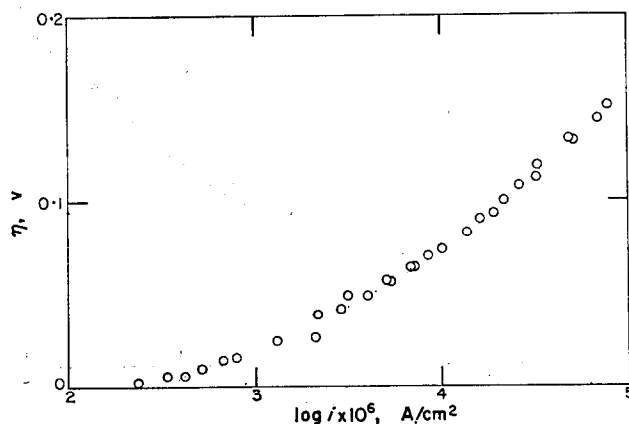


FIG. 3. Tafel plots for palladized-palladium electrodes, 323°C.
Results from different runs.

Data obtained from the Tafel plots are assembled in Table 1. $(b_T)_I$ and $(b_T)_{II}$ are the Tafel slopes ($\partial\eta/\partial(\log i)$); $(\Delta\eta)_I$ and $(\Delta\eta)_{II}$ are the overvoltage ranges of the Tafel lines and $\log(i_0)_I$ and $\log(i_0)_{II}$ are obtained by extrapolating the Tafel lines to $\eta = 0$. The i_0 's are the apparent exchange cds.

TABLE 1. KINETIC DATA FROM TAFEL PLOTS. PALLADIZED-PALLADIUM CATHODES

Temp °C	$(b_T)_I$ mV	$(\Delta\eta)_I$ mV	$(b_T)_{II}$ mV	$(\Delta\eta)_{II}$ mV	$\log(i_0 \times 10^9)_I$ (i_0 in A/cm ²)	$\log(i_0 \times 10^9)_{II}$ (i_0 in A/cm ²)	2.3RT/F mV
254(P)	70 ± 5	40-200	186 ± 5	200-500	0.65	2.55	104.6
254(G)	75	40-200	186	200-500	0.95	2.60	104.6
255(G)	58 ± 2	40-100	170 ± 5	160-400	1.35	2.77	104.8
255(P)	58	40-90	178	120-400	1.80	3.00	104.8
272(G)	56 ± 4	30-90	252 ± 5	120-350	2.45	3.80	108.2
272(G)	60	30-90	250	120-350	2.60	3.78	108.2
323(P)	51 ± 5	20-80	100 ± 5	80-160	2.58	3.35	118.3
323(G)	—	—	113	80-230	—	3.22	118.3

P, potentiostatic run.
G, galvanostatic run.

From the initial portion of the current/voltage curve, the stoichiometric number can be estimated as usual. Its value, in spite of a large error, is about 1, as for the same electrochemical process on gold electrodes.³

Decay curves cover from 10⁻⁵ up to 10 s, as shown in Fig. 4 by plotting the overvoltage against log (time). At times comprised between 10⁻⁵ and 10⁻² s, there is a region where the departure of the potential from the initial value is rather small. At

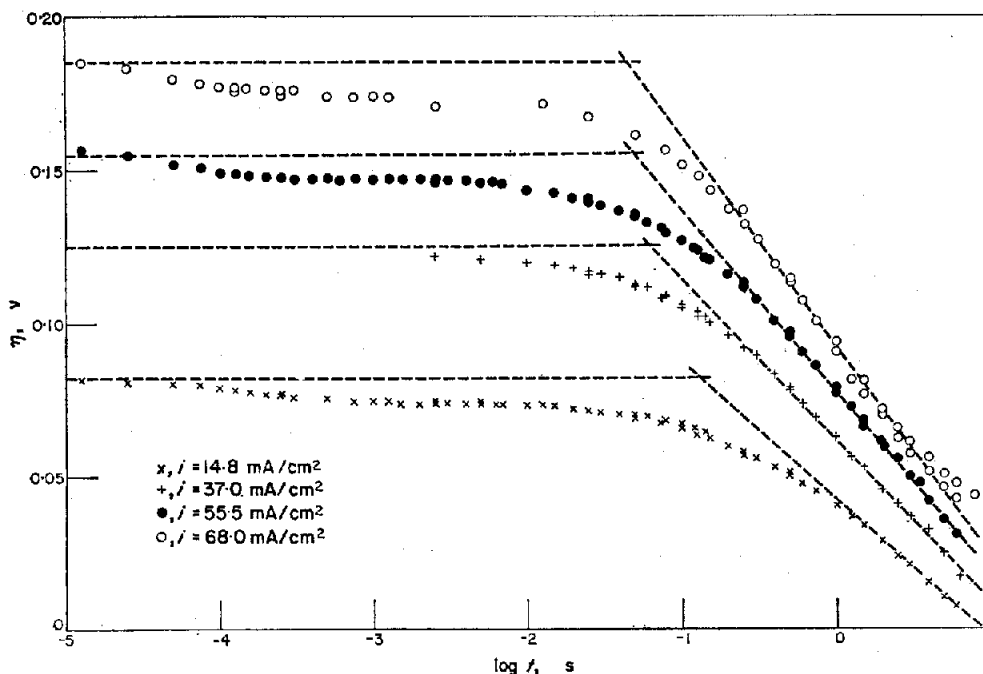


FIG. 4. Semilogarithmic plot of decay curves, 323°C. Palladized-palladium electrodes.

times over 10^{-1} s a linear portion is observed, particularly at the highest cds, covering about 0.1 V on the potential scale. The slope of this straight line $b_d = |\partial\eta/\partial(\log t)|$ depends on the initial potential and approaches a value close to $2.3(RT/2F)$.

From intersection of the decay slope and the horizontal line corresponding to the initial potential at current interruption, a $\log t'$ value was evaluated, related to the apparent electrode capacitance C by the expression $C = 2.3 i \times t'/b_d$, where b_d is the decay slope. Values of t' , b_d and C , for palladized-palladium electrodes, are shown in Table 2.

TABLE 2. DATA FROM DECAY CURVES. PALLADIZED-PALLADIUM CATHODES, 323°C

i mA/cm ²	b_d mV	t' s	C F/cm ²	$2.3RT/F$ mV
14.8	45 ± 4	0.126	0.095 ± 0.02	118.3
37.0	53	0.063	0.10	118.3
55.5	59	0.050	0.11	118.3
74.0	68	0.045	0.11	118.3

The experiments with palladized-palladium electrodes do not yield a clear dependence of the apparent electrode capacitance on overvoltage, as deduced from Table 2. However, its large value indicates an appreciable roughness of this type of electrode.

Palladized-platinum electrodes

Palladized-platinum electrodes were examined to avoid any interference in the kinetic measurements due to hydrogen dissolution in the base metal, as probably occurred with the palladized-palladium electrodes.

The current/voltage curves obtained with palladized platinum electrodes resemble very much those already described for palladized-palladium electrodes, as shown in Fig. 5 for experiments performed at 270°C. At low overvoltages the best straight line has a slope close to $2.3(RT/2F)$ whereas at high overvoltages a straight line with a slope approaching $2.3(RT/F)$ is observed.

At a higher temperature, there is an appreciable overvoltage decrease. In the best case, only one straight line portion can be drawn, as shown in Fig. 6; the slope is lower than $2.3(RT/F)$. Data obtained from current/voltage curves are assembled in Table 3.

Overvoltage decay in a semilogarithmic plot is presented in Fig. 7, for experiments at 272°C. At shorter times the change of potential is rather small. Thus, from 10^{-4} to 10^{-1} s, the overvoltage decays only about 0.01 V, for experiments at 0.046 A/cm². At higher cds a linear $\eta/\log t$ region exists, extending from about 1 s upwards, until the overvoltage reaches about 0.030 V. The slope of the straight line approaches $2.3(RT/2F)$.

The decay of cathodic overvoltage at higher temperature is similar to that observed at lower ones, Fig. 8. The straight line portion covers an overvoltage region from about 0.2 to 0.05 V, depending on cd and the slopes of the best straight lines are close to $2.3(RT/2F)$. Data deduced from decay curves is assembled in Table 4.

The electrode roughness is reflected in the large apparent electrode capacitance. There is a clear decrease of the electrode capacitance with increasing overvoltage.

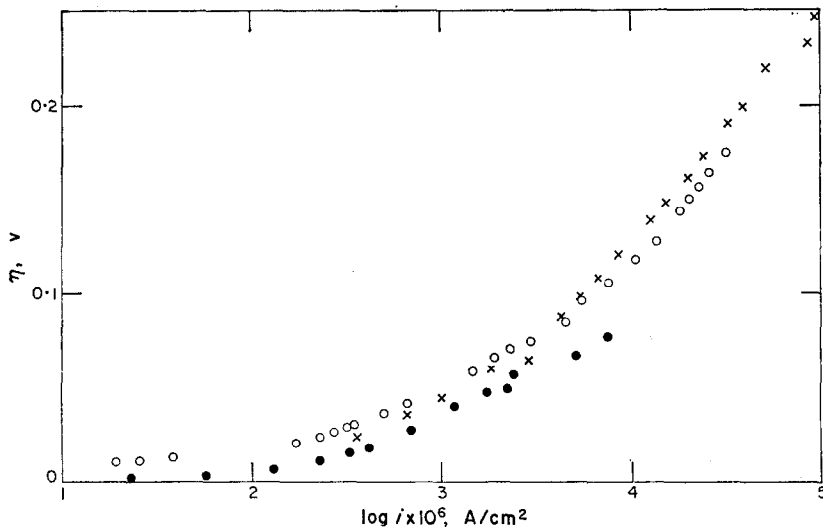


FIG. 5. Tafel plots for palladized-platinum electrodes, 270°C. Results from different runs. ●, increasing cd; ○, decreasing.

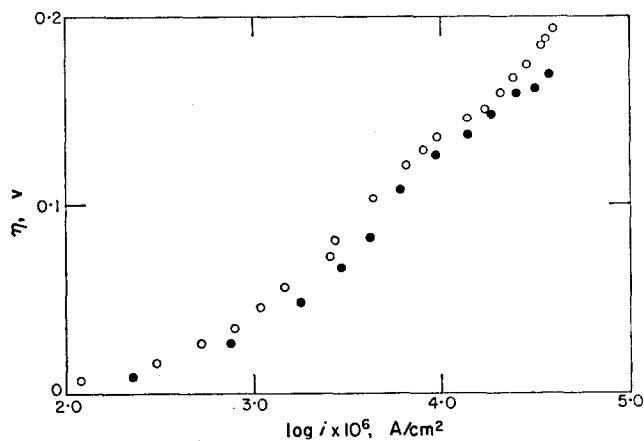


FIG. 6. Tafel plots for palladized-platinum electrodes, 317.5°C. Results from different runs. ●, increasing cd; ○, decreasing.

TABLE 3. KINETIC DATA FROM TAFEL PLOTS. PALLADIZED-PLATINUM CATHODES

Temp °C	$(b_T)_I$ mV	$(\Delta\eta)_I$ mV	$(b_T)_{II}$ mV	$(\Delta\eta)_{II}$ mV	$\log(i_0 \times 10^6)_I$ (i_0 in A/cm ²)	$\log(i_0 \times 10^6)_{II}$ (i_0 in A/cm ²)	$2.3RT/F$ mV
270(G)	44 ± 6	20-90	122 ± 5	90-250	1.84	2.99	107.8
270(P)	50 ± 6	20-90	122 ± 5	90-250	2.00	3.19	107.8
272(G)	52 ± 4	30-80	110 ± 5	90-150	2.50	3.26	108.2
276(G)	64 ± 5	30-80	105 ± 5	90-150	2.69	3.21	109.0
317.5(P)	91 ± 6	40-200	—	—	2.53	—	117.2
317.5(P)	89 ± 6	40-200	—	—	2.63	—	117.2

P, G, as Table 1.

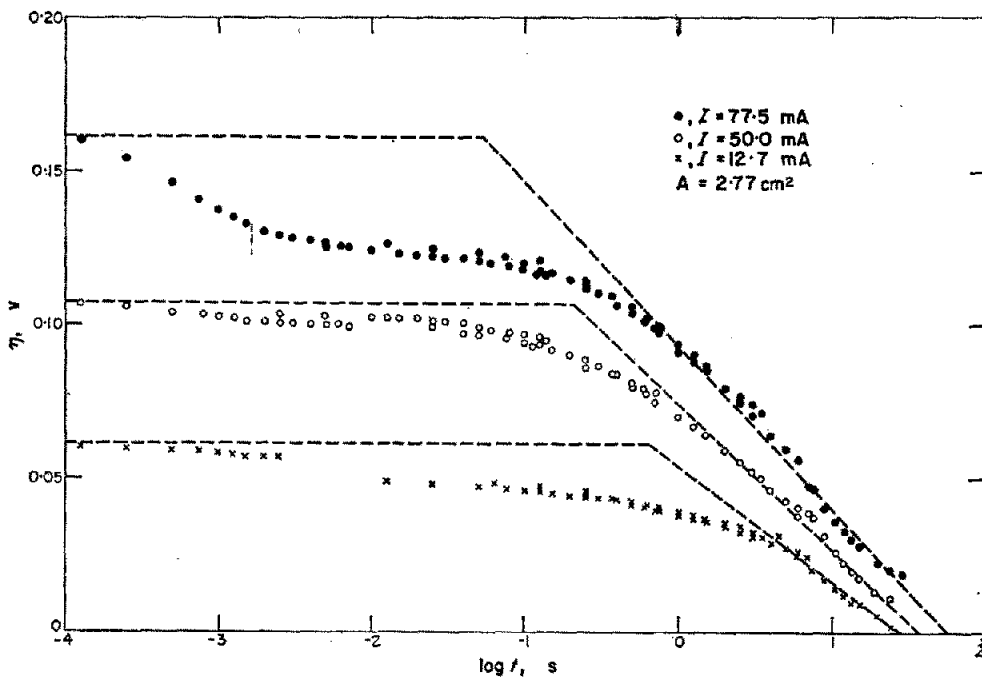


FIG. 7. Semilogarithmic plot of decay curves, 267°C. Palladized-platinum electrodes.

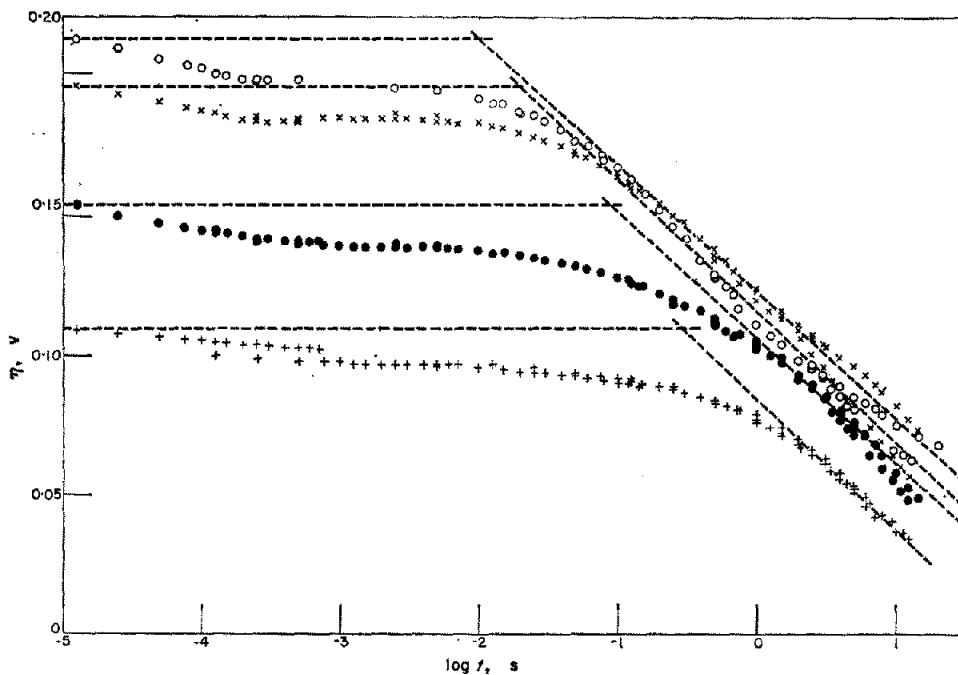


FIG. 8. Semilogarithmic plot of decay curves, 324°C. Palladized-platinum electrodes.

- + , $i = 6.45$ mA/cm²
- , $i = 13.9$ mA/cm²
- × , $i = 29.0$ mA/cm²
- , $i = 39.0$ mA/cm²

TABLE 4. DATA FROM DECAY CURVES. PALLADIZED-PLATINUM CATHODES

i mA/cm ²	b_d mV	$2.3RT/F$ mV	t' s	C F/cm ²
267°C				
4.58	40 ± 2	107.2	0.81	0.21 ± 0.02
18.1	47	107.2	0.29	0.26
20.0	54	107.2	0.17	0.14
28.0	54	107.2	0.054	0.060
272°C				
7.9	37 ± 2	108.2	0.37	0.18 ± 0.02
19.8	46	108.2	0.13	0.13
39.5	46	108.2	0.030	0.060
51.4	46	108.2	0.013	0.03
324°C				
6.45	48 ± 2	118.5	0.30	0.093 ± 0.005
13.9	48	118.5	0.089	0.059
29.0	48	118.5	0.020	0.028
39.0	47	118.5	0.010	0.019

Bright palladium cathodes

When bright palladium cathodes were used, the electrolyte was saturated either with hydrogen or with nitrogen. Figure 9 presents a Tafel plot under 1 atm pressure at low temperature. Hydrogen saturation was required to achieve stable open-circuit potentials particularly at low cds. In this region, although hydrogen saturation existed, the current/voltage curve exhibited a larger overvoltage when it was retraced with decreasing current.

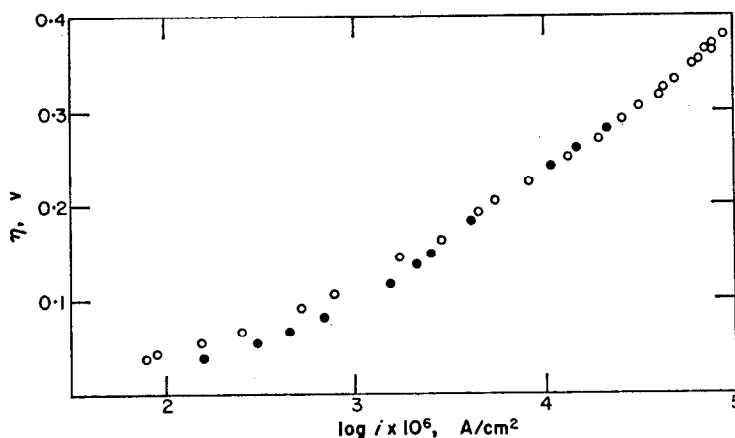


FIG. 9. Tafel plots for bright palladium electrodes, 267°C.
Results from different runs with hydrogen saturation.
●, increasing cd; ○, decreasing.

When the melt was continuously saturated with nitrogen, the open-circuit potential shifted towards more negative values and the shape of the current/voltage curve was also appreciably modified, as is shown in Fig. 10, as reflected in the apparent exchange-current-density values. Since nitrogen saturation shifts the electrode potential and

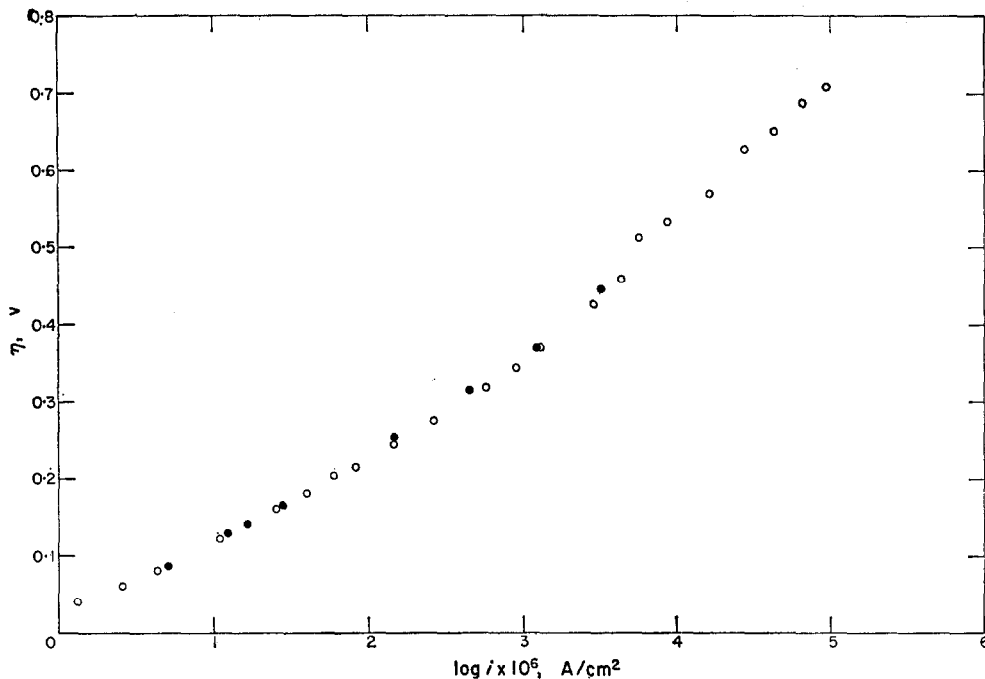


FIG. 10. Tafel plots for bright palladium electrodes, 243°C.
Results from different runs with nitrogen saturation.
●, increasing cd; ○, decreasing.

there is a simultaneous formation of hydrogen at rates depending on cd, those experiments are not easy to interpret. Indeed, a proper definition of the overvoltage at each cd and nitrogen flow rate is not possible.

The experimental data, in the overvoltage range from about 0.04 to 0.11 V, fit Tafel lines of slopes between $2.3(RT/2F)$ and $2.3(RT/F)$. At higher overvoltages a second Tafel line can be drawn the slope of which is lower than $2.3(2RT/F)$.

At higher temperatures, as shown in Fig. 11, the Tafel plot is linear from 0.03 to 0.11 V with a slope of about $2.3(RT/2F)$. No appreciable hysteresis effect is observed. The kinetic parameters deduced from the Tafel plots are assembled in Table 5.

Typical decay curves, at low temperatures are presented in Fig. 12 in a semi-logarithmic plot. Data fit a straight line from 10^{-4} to 1 s or thereabouts; the slope again approaches a value close to $2.3(RT/2F)$ at higher current. At times larger than 1 s, deviation from linearity is observed, particularly for experiments at high cds.

At higher temperatures the decay curves differ appreciably from those described before, as shown in Fig. 13. The semi-logarithmic plot indicates an interval between 10^{-5} up to about 10^{-2} s where the overvoltage decay is rather small. Beyond 10^{-2} s a second region is observed where the data fit a straight line, which at the highest cds has a slope close to $2.3(RT/2F)$, as already observed for the other electrodes at different temperatures.

When the electrode potential approaches the open-circuit value, deviation from linearity is again observed, which is actually expected, according to the theory of

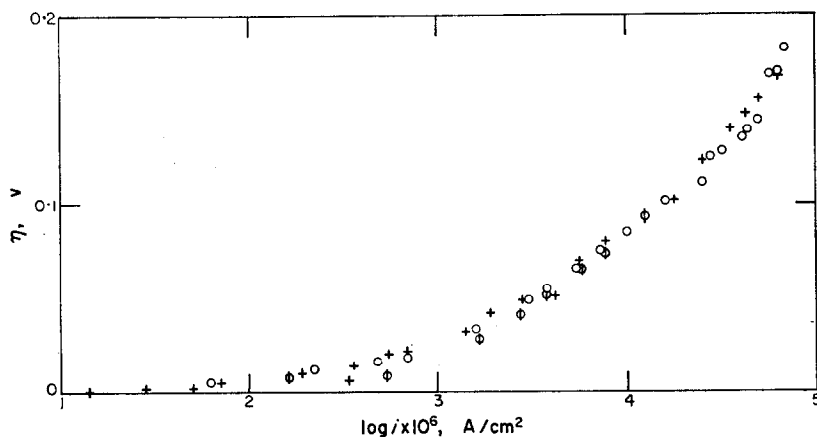


FIG. 11. Tafel plots for bright palladium electrodes, 322°C.
Results from different runs; O, potentiostatic run.

TABLE 5. KINETIC DATA FROM TAFEL PLOTS. BRIGHT PALLADIUM CATHODES

Temp °C	$(b_T)_H$ mV	$(\Delta\eta)_H$ mV	$(b_T)_{H1}$ mV	$(\Delta\eta)_{H1}$ mV	$\log(i_0 \times 10^6)$ (i_0 in A/cm ²)	$\log(i_0 \times 10^6)_{H1}$ (i in A/cm ²)	$2.3RT/F$ mV
242(P, N ₂)	84 ± 4	50–170	160 ± 5	160–500	0.23	1.03	102.2
243(P, N ₂)	113 ± 4	100–300	184 ± 6	320–700	0.00	1.10	102.4
243(P)	100 ± 2	40–140	174	140–550	0.07	0.68	102.4
244(P)	110 ± 5	80–180	165	200–600	0.01	0.60	102.6
265(P)	80 ± 10	40–160	146 ± 10	120–400	1.17	2.13	106.8
267(P)	50 ± 4	40–120	142 ± 6	120–360	1.45	2.33	107.2
273(P)	68 ± 5	40–120	189 ± 10	150–300	—	—	108.4
322(G)	68 ± 3	30–110	—	—	2.68	—	118.1
322(P)	67 ± 3	30–110	—	—	2.75	—	118.1

P, G, as Table 1.

electrode potential decay, after the current is switched off. Results obtained from decay curves with bright palladium electrodes are shown in Table 6.

Build-up curves

Build-up curves at constant current were measured in the μ s range at different cds, and from the initial slope the electrode capacitance at rest potential was evaluated as usual. The palladized-platinum electrodes exhibited an electrode capacitance of the order of 1000 to 1500 μ F/cm² over the whole temperature range.

Results obtained for bright palladium electrodes are assembled in Table 7. The experimental electrode capacitances at the rest potential at 330°C are larger than at 276°C.

The rest potential

The various kinds of palladium electrodes used exhibit a sufficiently stable and reproducible open-circuit potential measured against the reference electrode. Typical rest potentials are assembled in Table 8. At temperatures lower than $292 \pm 4^\circ\text{C}$, the palladium electrodes are more negative than the reference electrode, while at larger

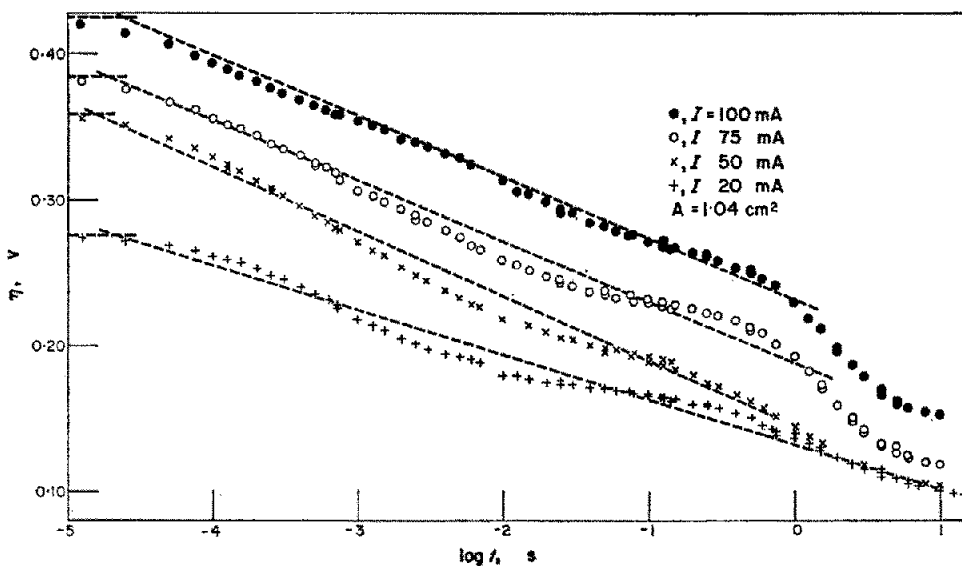


FIG. 12. Semilogarithmic plot of decay curves, 267°C. Bright palladium electrodes.

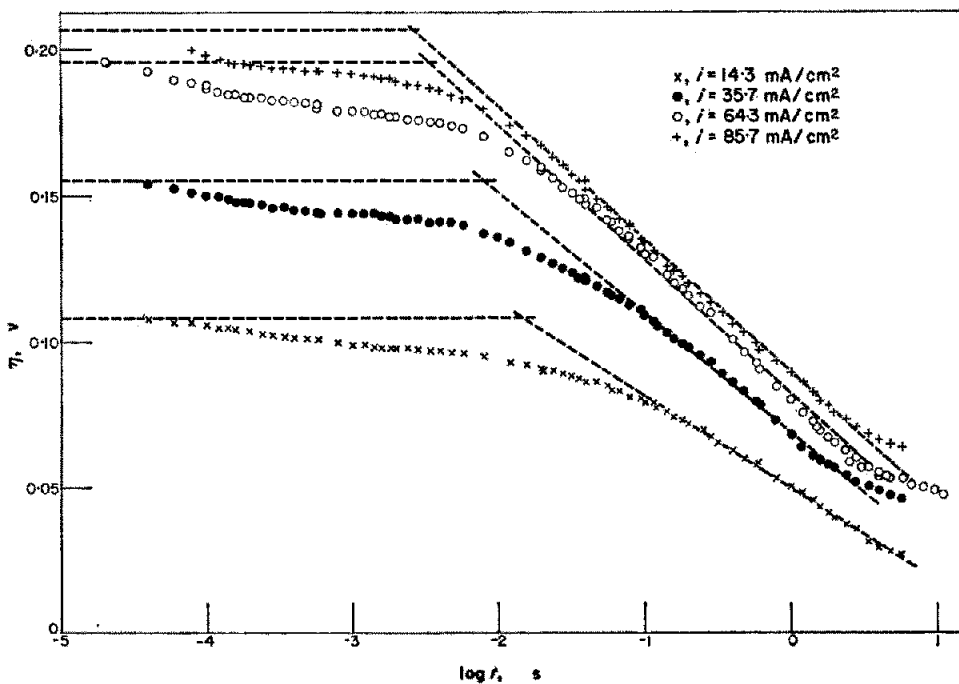


FIG. 13. Semilogarithmic plot of decay curves, 324°C. Bright palladium electrodes.

TABLE 6. DECAY FROM DECAY CURVES. BRIGHT PALLADIUM CATHODES

i mA/cm ²	b_a mV	t' s	C μF/cm ²	$2.3RT/F$ m ₊
267°C				
19.2	31 ± 3	2.2 × 10 ⁻⁵	31	109.0
48.0	44	1.5 × 10 ⁻⁵	38	109.0
72.0	42	1.7 × 10 ⁻⁵	67	109.0
96.0	41	2.3 × 10 ⁻⁵	124	109.0
324°C				
14.3	22 ± 3	14.5 × 10 ⁻³	21,700	119.7
35.7	42	7.94 × 10 ⁻³	15,500	119.7
64.3	47	3.24 × 10 ⁻³	10,020	119.7
85.7	46	2.88 × 10 ⁻³	12,300	119.7

TABLE 7. DATA FROM BUILD-UP CURVES. BRIGHT PALLADIUM CATHODES

i mA/cm ²	$(\partial i/\partial \eta)_{\eta \rightarrow 0}$ s/V	C μF/cm ²
276°C		
20	3.0 × 10 ⁻⁴	6.0 ± 2
51	1.33 × 10 ⁻⁴	6.8
75	0.91 × 10 ⁻⁴	6.8
330°C		
20	18.9 × 10 ⁻⁴	36 ± 7
40	9.6 × 10 ⁻⁴	33
80	3.4 × 10 ⁻⁴	28

TABLE 8. REST POTENTIALS OF PALLADIUM CATHODES
(AGAINST HYDROGEN REFERENCE ELECTRODE).

Temp °C	E_r mV
Palladized-palladium	
255	-129.6
255	-110.0
264	-68.0
272	-65.0
323	80.0
Bright palladium	
267	-77.5
267	-77.5
322	116.4
324	122.0

temperatures they become positive. Therefore at $292 \pm 4^\circ\text{C}$ the palladium-hydrogen electrode behaves as the platinum-hydrogen electrode in molten potassium bisulphate. The potential displayed by the palladium-hydrogen system with respect to the reference electrode shows no definite response to the type of palladium surface used.

DISCUSSION

The hydrogen-evolution reaction on the different palladium electrodes at lower temperatures is in principle characterized by at least three distinct regions in the steady

$\eta/\log i$ plot, similar to the behaviour of the α -Pd-hydrogen electrode in acid aqueous solutions at room temperature.²³ Initially there are two Tafel regions, the first having a slope of about $2.3(RT/2F)$ and the second a slope between $2.3(RT/F)$ and $2.3(2RT/F)$.

At higher temperatures the lower Tafel slope apparently predominates, although the overvoltage diminishes appreciably, so that the high-slope region may occur at overvoltages higher than those investigated.

In a general fashion these kinetic parameters resemble those already obtained for gold electrodes³ in bisulphate melts. As already discussed in that case, when adsorption of intermediates occurs during the electrode process, the elucidation of its kinetics based only on the kinetic data deduced from steady Tafel plots is not feasible. Thus, simple kinetic analysis of the electrode processes shows that the slopes $2.3(RT/2F)$ and $2.3(2RT/F)$ could represent definite mechanisms. The former corresponds to an electrochemical mechanism of consecutive step where the combination of atoms is rate control, whereas the latter is related either to the initial hydrogen-ion discharge reaction or to the ion-plus-atom reactions as rate-determining steps, assuming the same type of mechanism under extreme adsorption isotherm conditions.²⁸ Taking into account the Tafel slopes, the stable rest potential achieved after a rather long time from current interruption, the fact that at a certain temperature the electrode shows the same potential as the platinum-hydrogen electrode in the acid melt, the estimated stoichiometric number, and the previous results on the kinetics of the hydrogen-electrode reaction on platinum and gold in bisulphate melts, a mechanism based exclusively on the discharge step as rate-determining must in principle be discarded.

The non-steady measurements are all characterized by at least a linear region of the $\eta/\log t$ plot, which approaches, at the highest cds, $2.3(RT/2F)$. The lower the cd (lower initial overvoltage), the lower the decay slope.

Two distinct cases must be distinguished. First, the experiments with palladized electrodes, at low and high temperatures, present a relatively large t' value and consequently a large apparent electrode capacitance, which may involve a significant contribution due to the electrode roughness, as occurred with platinized-platinum and gilded-gold electrodes. However, assuming a constant roughness at a fixed temperature, the decrease of the apparent electrode capacitance with overvoltage may be explained, in principle, on the basis of an intermediate degree of coverage by hydrogen adatoms between 0.5 and 1.0, approaching the latter at high overvoltages, as deduced from the theory of electrode pseudo-capacitance.²⁸ In this case the decay slopes should be lower than $2.3(RT/2F)$, tending to the latter at higher overvoltages.

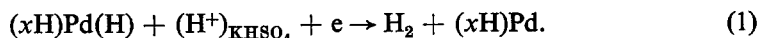
A second case is observed in the bright palladium electrodes. Although the decay slopes also approach $2.3(RT/2F)$, the overvoltage decay reaches the linear $\eta/\log t$ region at very short times, yielding in consequence a low t' value and an apparent electrode capacitance of a reasonable order of magnitude assuming a rather simple double layer structure. The experimental electrode differential capacitance shows in this case a steady increase with overvoltage but it is difficult to draw a definite conclusion from this dependence because of the probable interference of the permeation process of hydrogen in palladium, which adds a further complication to the structure of the reaction zone.

At higher temperatures, a remarkably longer time is required for reaching the

linear $\eta/\log t$ region. Thus t' is larger, and the apparent electrode differential capacitance increases by a factor between 10^2 to 10^3 as compared to the lower temperature experiments at the same cd, and it decreases as overvoltage increases, at least in a certain overvoltage region.

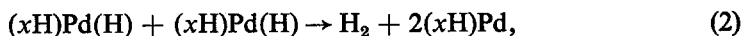
The fact that the slope $2.3(RT/2F)$ is always approached in the $\eta/\log t$ plot suggests that at least in most of the overvoltage region investigated, the decay process can be interpreted in terms of a reaction mechanism comprising the combination of hydrogen adatoms on the palladium surface as the rate-determining step, assuming that the intermediates obey either a Langmuir adsorption isotherm with negligible degree of surface coverage, which is unlikely, or a Temkin-type adsorption isotherm with an intermediate degree of surface coverage and non-activated adsorption of the adatoms in the electrode process.²⁸ It must be admitted that on the basis of the physico-chemical properties of the Pd-H systems,²⁹ a degree of coverage of the metal by hydrogen atoms approaching zero is most improbable.

If the electrode surface becomes completely covered by hydrogen atoms at a certain overvoltage, it is reasonable to expect that the reaction kinetics will be controlled by the ion-plus-atom discharge reaction,



This reaction at high degree of coverages yields a Tafel slope of $2RT/F$. This behaviour has been observed in palladium electrodes in aqueous solutions.³⁰

To explain the peculiar behaviour of the decay process in the whole range, let us assume then that the principal reaction is



where $(xH)Pd(H)$ is a hydrogen atom bound to the palladium-hydrogen electrode surface with the Pd/H atomic ratio is $1/x$. Let the rate of reaction (2) be indicated by v_r , so the kinetic equation related to hydrogen formation is

$$v_r = k_r \theta^2, \quad (3)$$

k_r being the specific rate constant and θ the degree of surface coverage, which is potential dependent.

After current interruption, the electrode overvoltage can keep a steady value if no change of the surface concentration of hydrogen adatoms occurs. One manner in which this can be achieved is by the transfer of hydrogen atoms from the bulk of the metal towards the electrode interface. This process is very likely to occur in the case of palladium where hydrogen permeation takes place easily. Therefore, the decay process at the electrode interface can be represented by the following simple model. At current interruption, two simultaneous processes occur, hydrogen-adatom consumption through reaction (2) and hydrogen diffusion from the bulk of the electrode to the reaction interface. Let us call the rate of the latter v_d .

The occurrence of both processes implies the discharge of the condenser formed at the interface, involving the capacitance of the electrical double layer. Therefore if the rate of discharge is given by v_{d1} ,

$$v_r - v_d = -v_{d1}. \quad (4)$$

According to the present results, if the electrode process gives an exchange cd i_0 and a Tafel slope $2.3(RT/2F)$, then at high overpotentials ($\eta > RT/2F$)

$$i_r = zFv_r = i_0 \exp \left[\frac{2F\eta}{RT} \right]. \quad (5)$$

The rate of hydrogen diffusion through palladium can also be expressed in terms of a cd. It is reasonable to assume simple linear diffusion towards the reaction interface, particularly for the planar electrodes. Thus

$$i_d = zFv_d = \frac{zFD_1^{1/2}C_1}{\pi^{1/2}t^{1/2}}, \quad (6)$$

where D_1 is the diffusion coefficient of hydrogen through the metal, C_1 the maximum concentration reached in the bulk of the metal and t the time elapsed since the interruption of the electrolysis current.

Since the rate of discharge of the electrical double layer $v_{d1} = C_{d1}d\eta/dt$, (4), with (5) and (6), gives

$$i_0 \exp \left[\frac{2F\eta}{RT} \right] - \frac{FD_1^{1/2}C_1}{\pi^{1/2}t^{1/2}} = -C_{d1} \frac{d\eta}{dt}. \quad (7)$$

Two limiting cases are distinguished in (7), namely, (i) $v_d \gg v_r$, and (ii) $v_d \ll v_r$.

If $v_r \gg v_d$, (7) becomes the equation already known for the discharge of the electrode capacitance by a faradaic process. Its integration, in the present circumstances, assuming that within the overvoltage range the electrode capacitance is constant, yields a linear $\eta/\log t$ relationship involving a slope $RT/2F$, corresponding to the steady $\eta/\log i$ plot.

When $v_d \gg v_r$, (7) becomes

$$\frac{FD_1^{1/2}C_1}{\pi^{1/2}t^{1/2}} = C_{d1} \frac{d\eta}{dt}. \quad (8)$$

Assuming that C_{d1} is also constant within the region of overvoltage change, integration of (8) yields

$$\frac{2FD_1^{1/2}C_1t^{1/2}}{C_{d1}\pi^{1/2}} = -\eta + \text{const.} \quad (9)$$

The integration constant becomes the overpotential at current interruption, if time t is the time elapsed since then.

When the rate of hydrogen diffusion is large as compared to the rate of the electrochemical reaction, (9) predicts a linear relationship between overvoltage and square root of time. This is actually satisfied by the experimental results obtained from decay curves at shorter times, as shown in Figs. 14 and 15 for differently prepared electrodes.

From the slopes of the $\eta/t^{1/2}$ plots it is possible now to estimate roughly the maximum concentration of hydrogen atoms into the palladium, at least for bright palladium electrodes, where any roughness effect may be neglected. The diffusion coefficient of hydrogen through α -Pd-H is taken from the literature;³¹ from 200 to 700°C, it is $D_1 = 4.3 \times 10^{-3} \exp(-5620/RT) \text{ cm}^2/\text{s}$. The actual electrode capacitance can be taken as 10^{-4} F/cm^2 , taking into account the contribution of a pseudo-capacitance due

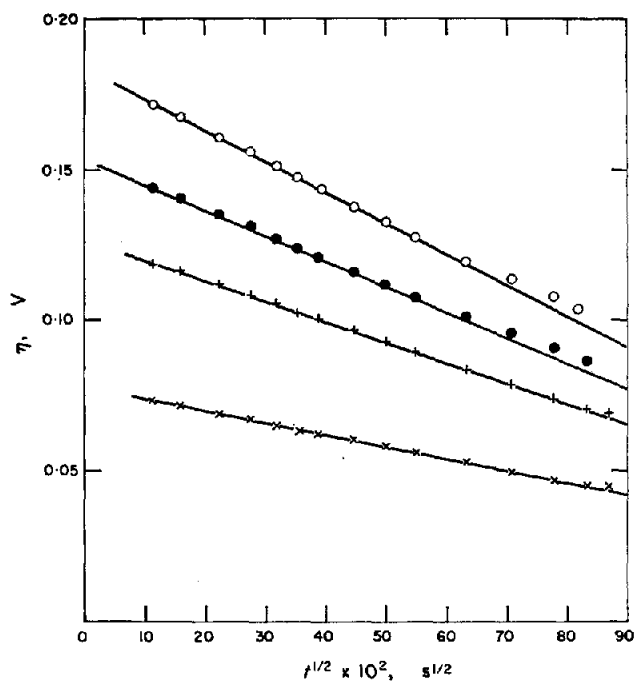


FIG. 14. Plot of η vs. $t^{1/2}$ of the initial portion of decay curves for palladized-palladium electrodes. 323°C.

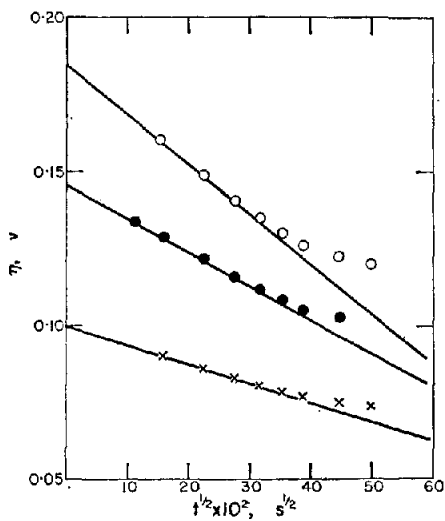


FIG. 15. Plot of η vs. $t^{1/2}$ of the initial portion of decay curves for bright palladium electrodes. 324°C.

to reaction intermediates. Data deduced from (9) for C_1 are given in Table 9. The concentration of hydrogen achieved in the palladium electrodes under the present circumstances is small as should be expected for the existence of a α -Pd-H phase under a 1 atm of hydrogen gas.³² The amount of dissolved hydrogen is as small as in platinum electrodes at lower temperatures, although its diffusion coefficient in the latter is very much smaller.³³

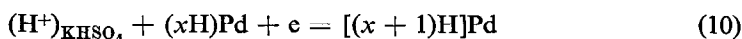
TABLE 9. MAXIMUM CONCENTRATION OF ATOMIC HYDROGEN IN BRIGHT PALLADIUM CATHODES AT 330°C

I mA	$\Delta\eta/\Delta t^{1/2}$ V/s ^{1/2}	C_1 g-atom/cm ³
20	0.062	0.92×10^{-4}
50	0.110	1.63×10^{-4}
90	0.160	2.37×10^{-4}

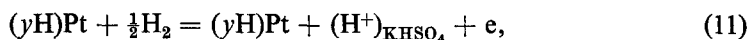
The fact that this effect is particularly noticeable on bright palladium at high temperature may be related to the form of kinetic law for the rate of hydrogen permeation. It was found that while the reaction order with respect to hydrogen gas pressure is about 1.2 to 1.3 at a temperature higher than 300°C, at 250°C it is about 0.7. It has also been observed that the process is strongly sensitive to the purity of the palladium.³⁴

Therefore, results from the decay process yield a clear support to the combination of adatoms as rate-determining step. This type of control seems to predominate in the intermediate overvoltage region of the steady current/voltage curves. The larger value of the electrode capacitance observed at high temperatures may also be related to the existence of a charge-distribution region extending into the metallic phase, assuming that absorbed hydrogen is dissociated into protons and electrons.³⁵

Let us now consider the residual potentials obtained a long time after current interruption following the procedure described for a Pd-H electrode at room temperature.³⁶ The discussion of the hydrogen-electrode process on palladium and its analogy with the process on platinum, at least in molten bisulphate, indicates that partial electrode processes occurring in the residual cell involving the palladium electrode and the reversible hydrogen electrode on platinum can be written



and



where x and y are the respective atomic ratios of H to metal in the palladium and platinum electrodes. There is good reason to believe that in aqueous media a reaction such as (10) takes place at the surface of the palladium-hydrogen alloy,³⁷ and reaction (11) also is reasonable on a hydrogen-saturated platinum electrode.³³ The sum of the two half reactions (10) and (11) yields the net reaction



and the free energy change, ΔG , may be written

$$\Delta G = \mu_{Pd} + (x+1)\mu_{H,Pd} - \frac{1}{2}\mu_{H_2,Pt} - \mu_{Pd} - x\mu_{H,Pd}, \quad (13)$$

where $\mu_{\text{H,Pd}}$, μ_{Pd} and $\mu_{\text{H}_2,\text{Pt}}$ are respectively the chemical potentials of hydrogen atoms in the metal lattice, of palladium atoms and of hydrogen molecules on platinum atoms. From (13),

$$\Delta G = \mu_{\text{H,Pd}} - \frac{1}{2}\mu_{\text{H}_2,\text{Pt}} \quad (14)$$

$\mu_{\text{H,Pd}}$ and $\mu_{\text{H}_2,\text{Pt}}$ are obtained only under equilibrium conditions. Then, the metal/hydrogen ratio should correspond to an equilibrium pressure. The following relationship must be satisfied,

$$\mu_{\text{H,Pd}} = \frac{1}{2}\mu_{\text{H}_2,\text{g}} \quad (15)$$

$\mu_{\text{H,g}}$ and $\mu_{\text{H}_2,\text{g}}$ are respectively the chemical potentials of hydrogen atoms in the hydrogen gas in equilibrium with the metal/hydrogen alloy and the chemical potential of hydrogen gas at the equilibrium pressure, p_e . Then, since

$$\mu_{\text{H,Pd}} = \mu_{\text{H,g}} = \frac{1}{2}\mu_{\text{H}_2,\text{g}} \quad (16)$$

using (14), (15) and (16) we have

$$\mu_{\text{H,Pd}} = \frac{\mu_{\text{H}_2,\text{Pd}}^\circ}{2} + \frac{RT}{2} \ln p_{e,\text{H}_2,\text{Pd}} \quad (17)$$

and

$$\mu_{\text{H}_2,\text{Pt}} = \mu_{\text{H}_2,\text{Pt}}^\circ + RT \ln p_{e,\text{H}_2,\text{Pt}} \quad (18)$$

From (14), (17) and (18)

$$\Delta G \approx \frac{RT}{2} \ln \frac{p_{e,\text{H}_2,\text{Pd}}}{p_{e,\text{H}_2,\text{Pt}}} \quad (19)$$

and the residual emf E_r is

$$E_r \approx \frac{RT}{2F} \ln \frac{p_{e,\text{H}_2,\text{Pt}}}{p_{e,\text{H}_2,\text{Pd}}} \quad (20)$$

Thus, at $292 \pm 4^\circ\text{C}$, near the critical point in the palladium/hydrogen system, the residual emf is zero and the equilibrium pressure of hydrogen atoms is equal on both palladium and platinum. A straightforward evaluation of the temperature dependence of the residual emf E_r , such as that performed for the Pd-H electrode at room temperature by various authors,^{36,38} is not feasible, as the temperature-dependence equations for the p_e for both metals are not available.

However, the fact that the palladium-hydrogen electrode displays a more positive potential at higher temperatures than the platinum-hydrogen electrode is a good indication of a more rapid decrease in hydrogen-atom concentration at the interphase as compared to platinum. This same effect is well known in the palladium-hydrogen system in aqueous solutions.^{36,39}

The temperature effect on the kinetics of the reaction is in the present case difficult to disentangle because not only the reaction rate changes but also the amount of hydrogen dissolved and the system itself changes with temperature. Taking into account that the α -phase of the palladium-hydrogen alloy is formed, no appreciable change of the electrode surface due to distention in the lattice parameter of pure palladium should occur. The lattice parameter of pure palladium is 3.883 Å, while that of the α -phase is 3.886 Å.

The conclusion reached from the present study is that the electrochemical formation of hydrogen on palladium electrodes previously treated as cathodes in the same melt occurs similarly to the reaction on active platinum electrodes, particularly at low overvoltage. A reproducible palladium-hydrogen electrode in molten bisulphate is also accomplished, as a consequence of the type of kinetics obeyed by the process. The α -palladium-hydrogen electrode formed in this case actually has a composition corresponding to that of the α -phase region, different from the α -palladium electrode at room temperature, which has a composition in the two-phase region. Here the potential is essentially independent of the H/Pd ratio. As already established by means of potential/composition data, at room temperature the electrode potential is dependent upon the composition of the electrode in the pure α -phase.^{35,40,41} This conclusion applies also to the palladium-hydrogen electrode in the molten bisulphates.

Acknowledgement—This work was done with partial financial aid from the C.N.I.C.T. of Argentina.

REFERENCES

1. H. A. VIDELA and A. J. ARVIA, *Electrochim. Acta* **10**, 21 (1965).
2. A. J. ARVIA, A. J. CALANDRA and H. A. VIDELA, *Electrochim. Acta* **10**, 33 (1965).
3. A. J. ARVIA, F. DE VEGA and H. A. VIDELA, *Electrochim. Acta* **13**, 581 (1968).
4. J. R. LACHER, *Proc. R. Soc.* **A161**, 525 (1937).
5. M. STACKELBERG and P. LUDWIG, *Z. Naturf.* **19a**, 93 (1964).
6. A. C. MAKRIDES, *J. phys. Chem.* **68**, 2160 (1964).
7. T. B. FLANAGAN, *Engelhard tech. Bull.* **VII**, 9 (1966).
8. J. P. HOARE, *J. electrochem. Soc.* **110**, 245 (1963).
9. M. FLEISCHMANN and H. R. THIRSK, *Trans. Faraday Soc.* **51**, 71 (1955).
10. D. J. G. IVES and G. J. JANZ, *Reference Electrodes*, p. 111. Academic Press, New York (1961).
11. A. SIEVERTS and H. BRÜNING, *Z. phys. Chem.* **A163**, 409 (1932).
12. A. SIEVERTS, H. HAGEN, *Z. phys. Chem.* **A174**, 247 (1935).
13. A. SIEVERTS, G. ZAPF, *Z. phys. Chem.* **A174**, 359 (1935).
14. D. P. SMITH, *Hydrogen in Metals*, p. 84. University of Chicago, Chicago (1948).
15. A. MAELAND and T. B. FLANAGAN, *J. phys. Chem.* **68**, 1419 (1964).
16. A. N. FRUMKIN, *Advances in Electrochemistry and Electrochemical Engineering*, ed. P. DELAHAY and C. W. TOBIAS. Wiley, New York (1963).
17. R. CLAMROTH and C. A. KNORR, *Z. Elektrochem.* **57**, 399 (1953).
18. L. KANDLER, C. A. KNORR and E. SCHWITZER, *Z. phys. Chem.* **A180**, 281 (1937).
19. C. A. KNORR, *Z. Elektrochem.* **59**, 647 (1955).
20. J. C. BARTON and F. A. LEWIS, *Z. phys. Chem.* **N.F. 33**, 101 (1962).
21. J. C. BARTON, W. F. N. LEITCH and F. A. LEWIS, *Trans. Faraday Soc.* **59**, 1208 (1963).
22. J. A. S. GREEN and F. A. LEWIS, *Trans. Faraday Soc.* **60**, 2234 (1964).
23. J. P. HOARE and S. SCHULDINER, *J. electrochem. Soc.* **104**, 564 (1964).
24. R. BARDE and R. BUVET, *J. Chim. phys.* **1365** (1963).
25. G. G. ARKHIPOV, L. P. KLEVTSOV and G. K. STEPANOV, *Tr. Inst. Elektrokhim. Akad. Nauk SSSR, Ural'sh Filial* **8**, 113 (1966); *C.A.* **65**, 16498 (1966).
26. H. BRODOWSKY, *Z. phys. Chem.*, **N.F. 44**, 129 (1965).
27. R. G. BATES, *Electrometric pH determinations*. Wiley, New York (1954).
28. B. E. CONWAY, *Theory and Principles of Electrode Processes*, p. 92. Ronald Press, New York (1965).
29. J. G. ASTON, *Engelhard tech. Bull.* **VII**, 14 (1966).
30. B. E. CONWAY, *Proc. R. Soc.* **A256**, 128 (1960).
31. A. C. MAKRIDES and D. N. JEWETT, *Engelhard Tech. Bull.* **VII**, 51 (1966).
32. L. J. GILLESPIE and L. S. GALSTAUN, *J. Am. chem. Soc.* **58**, 2565 (1936).
33. E. GILEADI, M. A. FULLENWIDER and J. O'M. BOCKRIS, *J. electrochem. Soc.* **113**, 926 (1966).
34. A. A. RODINA and N. I. DORONICHEVA, *Zh. fiz. Khim.* **40**, 1450 (1966).
35. C. WAGNER, *Z. phys. Chem.* **A193**, 386 (1944).
36. M. VASILE and C. G. ENKE, *J. electrochem. Soc.* **112**, 865 (1965).
37. T. B. FLANAGAN and F. A. LEWIS, *Trans. Faraday Soc.* **56**, 363 (1960).
38. R. J. RATCHFORD and G. W. CASTELLAN, *J. phys. Chem.* **62**, 1123 (1958).
39. J. BÉNARD, *C.r. hebd. Séanc. Acad. Sci., Paris* **218**, 967 (1944).
40. T. B. FLANAGAN and F. A. LEWIS, *Trans. Faraday Soc.* **55**, 1409 (1959).
41. P. C. ABEN and W. G. BURGER, *Trans. Faraday Soc.* **58**, 1989 (1962).